ADVANCED FUNCTIONAL MATERIALS
www.afm-journal.de

Short Synthetic β-Sheet Forming Peptide Amphiphiles as Broad Spectrum Antimicrobials with Antibiofilm and Endotoxin Neutralizing Capabilities

*Zhan Yuin Ong, Shu Jun Gao, and Yi Yan Yang**

Although naturally occurring membrane lytic antimicrobial peptides (AMPs) and their analogs hold enormous promise for antibiotics-resistant infectious disease therapies, significant challenges such as systemic toxicities, long peptide sequences, poor understanding of structure-activity relationships, and the potential for compromising innate host defense immunity have greatly limited their clinical applicability. To improve the clinical potential of AMPs, a facile approach is adopted to design a series of short synthetic β-sheet folding peptide amphiphiles comprised of short recurring $(X_1Y_1X_2Y_2)_n$-NH_2 sequences, where X_1 and X_2: hydrophobic residues (Val, Ile, Phe or Trp), Y_1 and Y_2: cationic residues (Arg or Lys), and n: number of repeat units; with systematic variations to the cationic and hydrophobic residues to obtain optimized AMP sequences bearing minimal resemblance to naturally occurring sequences. The designed β-sheet forming peptides exhibit broad spectrum antimicrobial activities against various clinically relevant microorganisms, including Gram-positive *Staphylococcus epidermidis* and *Staphylococcus aureus*, Gram-negative *Escherichia coli* and *Pseudomonas aeruginosa*, and yeast *Candida albicans*, with excellent selectivities for microbial membranes. Optimal synthetic peptides with n = 2 and n = 3 repeat units, i.e., $(IRIK)_2$-NH_2 and $(IRVK)_3$-NH_2, efficiently inhibit sessile biofilm bacteria growth leading to biomass reduction. Additionally, sequences with n = 3 repeat units effectively neutralize endotoxins while causing minimal cytotoxicities. Taken together, these findings clearly demonstrate that the rationally designed synthetic β-sheet folding peptides are highly selective, non-cytotoxic at antimicrobial levels and have tremendous potential for use as broad spectrum antimicrobial agents to overcome multidrug resistance in a wide range of localized, systemic, or external therapeutic applications.

1. Introduction

Despite significant improvements in living standards and biomedical technologies over the past century, the global burden of infectious diseases remains exceedingly high and is a major cause of public health, economic and social problems. According to World Health Organization (WHO) statistics, infectious and parasitic diseases such as pneumonia, tuberculosis, meningitis, diarrhoeal diseases, HIV and malaria are the second leading causes of death worldwide.[1] The widespread and often indiscriminate use of antibiotics in industrialized nations further fuels the problem by contributing to the rapid emergence of drug resistant pathogens, making infectious diseases increasingly difficult to control with the existing classes of antibiotics. Concomitantly, the complex pathophysiological processes involved in many infectious diseases such as those related to biofilm formation and bloodstream infections further contribute to the infectious disease treatment conundrum. Biofilm formation, which occurs when microbial cells adhere to each other and become embedded in a matrix of extracellular polymeric substance (EPS) on a surface, has been implicated in a variety of chronic microbial infections.[2,3] The eradication of biofilms presents as an immense medical challenge due to the poor penetration of antibiotics through the EPS and/or their inactivation by components of the EPS, often giving rise to the rapid development of antibiotic resistance. Similarly, in the treatment of nosocomial or community acquired bloodstream infections (e.g., sepsis or bacteremia), the rising prevalence of drug resistant microbes such as methicillin-resistant *Staphylococcus aureus* (MRSA), multidrug-resistant *Pseudomonas aeruginosa* and vancomycin-resistant *Enterococci* (VRE) remains a major clinical challenge.[4] Additionally, satisfactory microbicidal agents that can simultaneously kill or inhibit microbes and neutralize the noxious immunostimulatory endotoxins liberated to alleviate septic shock syndrome are acutely lacking.[5]

The mounting crisis of antibiotic-resistant infections coupled with the ongoing dearth in new small-molecule antibiotics development,[6] have spurred considerable efforts toward the discovery and development of membrane active antimicrobial peptides (AMPs) as an alternative class of antimicrobial agents. Unlike conventional antibiotics that inhibit specific biosynthetic pathways such as cell wall or protein synthesis, the majority of

Dr. Z. Y. Ong, S. J. Gao, Prof. Y. Y. Yang
Institute of Bioengineering and Nanotechnology
31 Biopolis Way, The Nanos
Singapore 138669, Singapore
E-mail: yyyang@ibn.a-star.edu.sg

DOI: 10.1002/adfm.201202850

the amphiphilic AMPs exert their activities via physical disruption of the more negatively charged microbial membrane lipid bilayers to induce leakage of cytoplasmic components leading to cell death.[7] The physical nature of membrane disruption is believed to result in a lower likelihood for drug resistance development as it becomes metabolically 'costlier' for the microorganism to mutate or to repair its membrane components at the same rate as the damage is being inflicted.

Although more than 1700 naturally occurring AMPs from diverse sources including microorganisms, plants and animals have been isolated and characterized in the past 3 decades,[8] only very few AMPs such as polymyxins and gramicidins are being used clinically; and their usage is mainly in topical formulations due to their high systemic toxicities.[9] In efforts to enhance antimicrobial activities and minimize non-specific toxicities, more researchers are increasingly utilizing naturally occurring AMP or protein sequences as templates to perform chemical modifications such as cyclization,[10] sequence truncations,[11] and substitution with D-,[12] β-[13] or fluorinated-amino acids[14] for the generation of new peptide analogs with broader applications. Current approaches to optimize naturally occurring AMP sequences, however, remain largely empirical at best, making it extremely difficult to delineate general structure-activity relationships especially against the backdrop of massive sequence and structural diversities. Furthermore, many of the new peptide analogs remain long (20 amino acids or more), which might induce significant immunogenicity and ultimately increase the cost for large scale manufacturing. More importantly, it has been suggested that the use of AMPs with sequences that are too close to the host defense AMPs may trigger the development of resistance towards innate AMPs that could inevitably compromise natural defenses against infections, posing significant health and environmental risks.[15]

The design and optimization of short synthetic peptides with minimal resemblance to naturally occurring peptide sequences is thus expected to be a useful strategy for the development of safe and efficacious AMPs for clinical use. While considerable efforts have been made to study the antimicrobial and hemolytic effects of charge, hydrophobicity and amphipathicity modifications in α-helical peptide sequences,[16–18] systematic studies involving β-sheet forming peptides remain somewhat lacking in comparison. More importantly, linear amphipathic β-sheet folding peptides have been found to possess greater selectivities toward microbial cell membranes when compared with their α-helical counterparts of equal charge and hydrophobicity.[19] Therefore, in this study, we adopted a facile approach to design a series of short synthetic β-sheet folding AMPs consisting of short recurring $(X_1Y_1X_2Y_2)_n$-NH_2 sequences based upon several basic design principles gleaned from naturally occurring β-sheet folding AMPs including: 1) the common occurrence of amphipathic dyad repeats in membrane-spanning β-sheets,[20] 2) the requirement for hydrophobic (X_1 or X_2 = Val and/or Ile or Phe or Trp) and cationic (Y_1 or Y_2 = Arg or Lys) residues to interact and perturb microbial cell walls and membranes, and 3) the strong β-sheet folding propensities reported for Val, Ile, Phe and Trp in the literature (**Scheme 1**).[21–23] As it was reported that C-terminal amidation enhanced antimicrobial activities due to the reinforcement of cationic character,[10,24] the peptides designed for this study were amidated at the C-terminal to confer a high net positive charge. Unlike most existing β-sheet AMPs, the designed

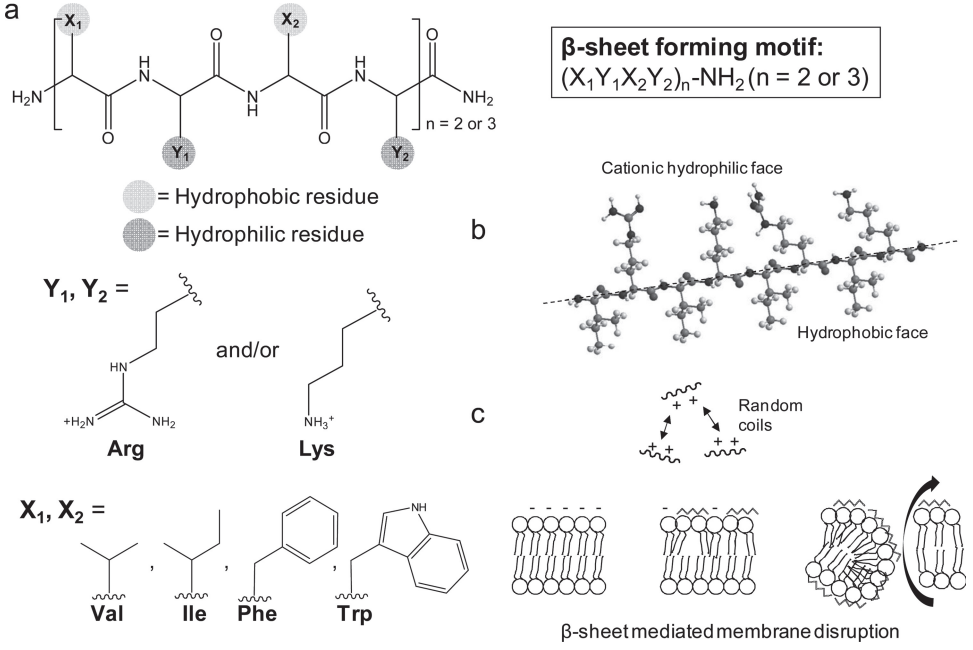

Scheme 1. Design of synthetic β-sheet forming antimicrobial peptides. a) Amphiphatic dyads of hydrophilic and hydrophobic amino acid residues. b) Orientation of cationic and hydrophobic amino acid residues on opposite faces of peptide molecule. c) Formation of β-sheet structures via electrostatic attraction of positively charged peptide sequences to negatively charged phospholipid membrane surface, followed by insertion of hydrophobic amino acid residues into the lipid bilayer to result in microbial membrane disruption and cell death.

Table 1. Synthetic β-sheet forming peptide designs and molecular weight characterizations.

No. of repeat units [n]	Repeat unit	Peptide sequence	Theoretical M_w	Observed M_w[a)]
2	VRVK	VRVKVRVK-NH_2	982.28	984.22
	IRIR	IRIRIRIR-NH_2	1094.42	1096.77
	IKIK	IKIKIKIK-NH_2	982.37	984.00
	IRIK	IRIKIRIK-NH_2	1038.39	1040.16
	IRVK	IRVKIRVK-NH_2	1010.34	1012.06
	FRFK	FRFKFRFK-NH_2	1174.46	1176.46
	WRWK	WRWKWRWK-NH_2	1330.61	1333.59
3	VRVK	VRVKVRVKVRVK-NH_2	1464.91	1467.16
	IRIK	IRIKIRIKIRIK-NH_2	1549.07	1551.43
	IRVK	IRVKIRVKIRVK-NH_2	1506.99	1510.43

[a)]Measured by MALDI-TOF MS, apparent $M_w = [M_w + H]^+$

peptides are short, linear and do not require disulfide bridges or cyclization for the stabilization of secondary structure or for antimicrobial activities,[9,25] which could reduce the cost in large scale production of the peptides. In aqueous solutions, the peptides are expected to exist as monomers due to electrostatic repulsion between the protonated Arg and/or Lys residues. In the presence of microbial cell membranes, the peptides readily fold into secondary β-sheet structures stabilized by electrostatic interactions between the positively charged residues and the negatively charged phospholipids, followed by the insertion of their hydrophobic residues into the lipid bilayer. Three important parameters including: 1) choice of cationic amino acid residue (i.e., Arg vs. Lys vs. combination of both), 2) degree of polarity and bulkiness of the hydrophobic side chain, and 3) length of peptide sequence were systematically investigated for effects on antimicrobial and hemolytic activities. The incorporation of both Arg and Lys cationic amino acid residues in our peptide designs was intended to capitalize on the high charge density of Arg for improving antimicrobial effects while tuning their selectivities using the less toxic Lys residue.[16,26]

The effectiveness of the synthetic β-sheet forming peptides against clinically relevant microorganisms and in challenging biomedical applications including the eradication of pre-formed biofilms and endotoxin neutralization were evaluated in relation to their toxicities. AMPs designed in this study were demonstrated to possess excellent antimicrobial activities and selectivities, effective biofilm dispersal and endotoxin neutralization properties. Therefore, they hold significant promise for the improved treatment of biofilm-related and/or bloodstream infections.

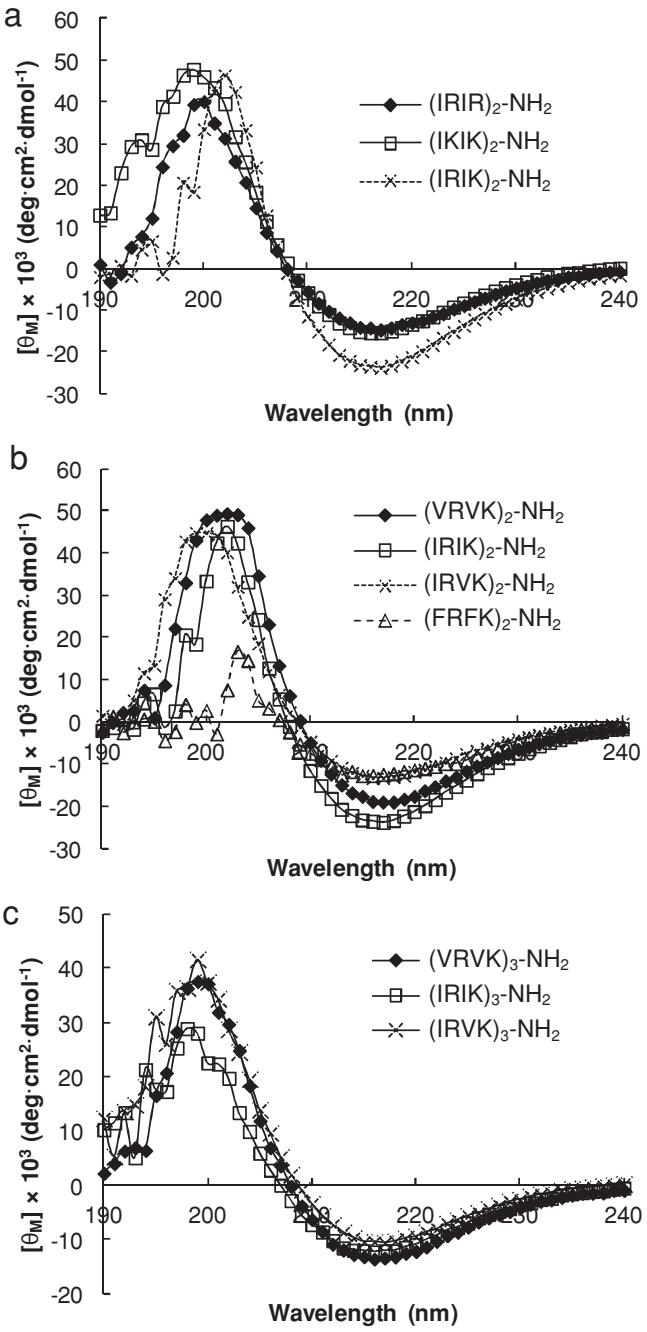

Figure 1. CD spectra demonstrating β-sheet formation of synthetic antimicrobial peptides with a) different cationic residue combinations (n = 2 repeat units), b) increasing hydrophobicity (n = 2) and (c) longer repeat units (n = 3) in membrane-mimicking environment (25 mM SDS micelles solution).

2. Results and Discussion

2.1. Peptide Design and Characterization

In this study, short amphiphilic peptides containing 8 or 12 amino acid residues were designed by segregating the cationic lysine and/or arginine amino acids in the polar face and various hydrophobic amino acids in the opposite non-polar face. The molecular weights of the synthesized peptides were verified by MALDI-TOF mass spectrometry and the observed molecular weights are listed in **Table 1**. It can be seen that the experimentally determined molecular weights were in close agreement with the calculated masses, indicating that the products correspond to the designed compositions.

Table 2. Minimum inhibitory concentrations (MICs) and therapeutic indices of synthetic antimicrobial peptides.

Antimicrobial peptide	MIC [mg L^{-1}]					GM[a] [mg L^{-1}]	HC_{10}[b] [mg L^{-1}]	SI[c]
	S. epidermidis	*S. aureus*	*E. coli*	*P. aeruginosa*	*C. albicans*			
$(VRVK)_2$-NH_2	62.5	> 500	250	> 500	15.6	–	>2500	>10[d]
$(IRIR)_2$-NH_2	3.9	31.3	7.8	7.8	15.6	13.3	150	11.3
$(IKIK)_2$-NH_2	2.0	125	31.3	31.3	2.0	38.3	700	18.3
$(IRIK)_2$-NH_2	3.9	62.5	15.6	31.3	3.9	23.4	1050	44.8
$(IRVK)_2$-NH_2	7.8	250	62.5	62.5	7.8	78.1	>2500	>32.0
$(FRFK)_2$-NH_2	7.8	250	15.6	62.5	62.5	79.7	1600	20.1
$(WRWK)_2$-NH_2	7.8	62.5	15.6	125	250	92.2	1000	10.8
$(VRVK)_3$-NH_2	1.0	62.5	15.6	62.5	31.3	34.6	>2500	>72.3
$(IRIK)_3$-NH_2	1.0	62.5	125	500	125	162.7	500	3.1
$(IRVK)_3$-NH_2	2.0	31.3	15.6	62.5	125	47.3	1250	26.4
Polymyxin B	15.6	125	2.0	2.0	62.5	41.4	>2500	>60.4

[a]Geometric mean (GM) of MIC values for the 5 microorganisms tested; [b]Hemolysis concentration 10% (HC_{10}) is defined as the lowest peptide concentration that induces ≥ 10% hemolysis; [c]Selectivity index (SI) is calculated as $\frac{HC_{10}}{GM}$; [d]Calculated as 2500 divided by 250 mg L^{-1}.

In deionized water, each peptide adopted a random coil structure that is characterized by a minimum at ≈198 nm in aqueous solutions due to intermolecular electrostatic repulsion between the protonated lysine and/or arginine residues (Supporting Information Figure S1). Under microbial membrane-mimicking hydrophobic environments (using 25 mM SDS micelles solution),[27] however, the synthetic peptides readily self-assembled into β-sheet secondary structures with characteristic CD spectra showing a maximum at ≈200 nm and minimum at ≈218 nm (**Figure 1**). The peptide $(WRWK)_2$-NH_2 did not give a discernible signal due to significant absorbance in the far ultraviolet region by the indole ring present in the Trp residues.

2.2. Antimicrobial Activities, Selectivities and LD50

The antimicrobial activities of the synthetic peptides and polymyxin B were tested against a representative set of clinically relevant microorganisms including Gram-positive *Staphylococcus epidermidis* and *Staphylococcus aureus*, Gram-negative *Escherichia coli* and *Pseudomonas aeruginosa*, and yeast *Candida albicans*. As shown in **Table 2**, the designed peptides displayed broad spectrum antimicrobial activities against the panel of microorganisms tested with geometric mean (GM) minimum inhibitory concentrations (MICs) ranging from 13.3 to 162.7 mg L^{-1}. Overall, the peptide $(IRIR)_2$-NH_2 for which all the cationic residues were Arg exhibited the best antimicrobial activities, with the lowest GM MIC value of 13.3 mg L^{-1}. This was followed closely by $(IRIK)_2$-NH_2 and $(IKIK)_2$-NH_2, with GM MIC values of 23.4 and 38.3 mg L^{-1}, respectively. As can be seen from these results, the peptide with 2 Arg and 2 Lys residues gave rise to antimicrobial effects that were in between its 4 Arg or 4 Lys counterparts. Next, we systematically varied the non-polar amino acids reported to possess high β-sheet forming propensities based on increasing degree of hydrophobicity[17] and bulkiness while retaining the combination of 2 Arg and 2 Lys cationic residues in peptide sequences containing n = 2 repeat units (Table 1). Among the peptides incorporating Val, Ile, Phe and Trp, the Ile-containing $(IRIK)_2$-NH_2 demonstrated the most effective antimicrobial activities against the panel of 5 microorganisms tested. The substitution of the second hydrophobic Ile residue in the peptide repeat unit with Val to give $(IRVK)_2$-NH_2 resulted in a notable decrease in antimicrobial activities from the original GM MIC value of 23.4 to 78.1. This result strongly suggests that the Ile residues were essential for the strong antimicrobial effects observed in peptides with n = 2 repeat units. The antimicrobial effects of the peptides with n = 3 repeat units were further investigated with sequences containing Val and Ile. As shown in Table 2, $(VRVK)_3$-NH_2 and $(IRVK)_3$-NH_2, but not $(IRIK)_3$-NH_2, demonstrated enhanced antimicrobial activities against *S. epidermidis*, *S. aureus* and *E. coli* when compared to their n = 2 counterparts, which could be attributed to the greater degree of bacterial membrane interaction and perturbation mediated by the longer n = 3 peptide sequences. The reduction in antimicrobial activities observed for the IRIK-containing peptides when n was increased from 2 to 3 could be due to the slight precipitation of $(IRIK)_3$-NH_2 in the growth medium at higher concentrations. Interestingly, the increase in peptide length resulted in a drastic reduction in activities against *C. albicans* suggesting that the short peptides with n = 2 repeat units were more active at interacting and disrupting the ergosterol-containing phospholipid membrane of fungal cells. In comparison to the clinically used lipopeptide polymyxin B, several of the β-sheet forming peptides, including $(IRIR)_2$-NH_2, $(IKIK)_2$-NH_2, $(IRIK)_2$-NH_2 and $(VRVK)_3$-NH_2 were found to have a wider spectrum of antimicrobial activities as seen from their lower GM MIC values (13.3 - 34.6 *vs.* 41.4).

For the designed β-sheet forming peptides to qualify as suitable therapeutic candidates, their antimicrobial activities should be considered in the light of their selectivities for the anionic microbial cell membranes over the zwitterionic mammalian cell membranes. As shown in **Figure 2**, the synthetic peptides induced minimal or no hemolysis against rat red blood cells at

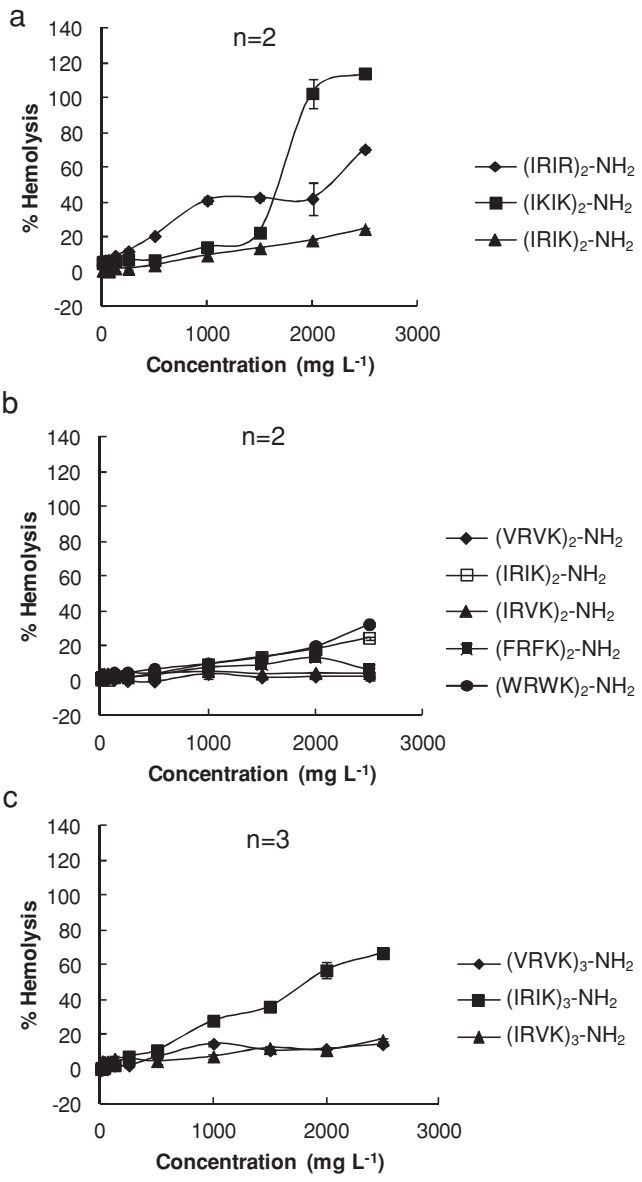

Figure 2. Hemolytic properties of the designed β-sheet forming peptides with a) different cationic residue combinations (n = 2 repeat units), b) increasing hydrophobicity (n = 2) and c) longer repeat units (n = 3) against rat red blood cells. All designed antimicrobial peptides induced minimal or no hemolysis at the concentrations required for antimicrobial activities.

various MIC values. We further evaluated the selectivity indices (SIs) of the peptides as a comparison of the safety and efficacies between various peptide sequences (Table 2). SIs of the various peptides were calculated as the ratio of the HC_{10} value (defined as the lowest peptide concentration that induces 10% or more hemolysis) to the GM (geometric mean MICs of the 5 microbial strains tested). HC_{10} value was used in this study as it is a more stringent measure of hemolytic activities as compared to the conventional HC_{50} values commonly cited in the literature. With the exception of $(IRIK)_3$-NH_2, all of the peptides tested were found to have high SIs of greater than 10, indicating that they have potential for both external and systemic applications in the body. In particular, we found that in peptides with n = 2 repeat units, the combination of both Arg and Lys residues in $(IRIK)_2$-NH_2 led to marked improvements in the SI from 11.3 and 18.3 of the single cationic amino acid peptide sequences $(IRIR)_2$-NH_2 and $(IKIK)_2$-NH_2, respectively to a value of 44.8. Among peptides with n = 3 repeat units, $(VRVK)_3$-NH_2, due to its relatively higher antimicrobial properties and low hemolytic properties, was found to have the highest SI of >72.3, which was followed by $(IRVK)_3$-NH_2 and $(IRIK)_3$-NH_2. Although polymyxin B was found to have relatively higher SI of >60.4 as compared to most of the synthetic β-sheet forming peptides due to its low hemolytic properties (Table 2),[28] its systemic application has been associated with other dose-limiting toxicities such as nephrotoxicity and neurotoxicity.[29] Thus, we proceeded to evaluate the acute systemic toxicity of several designed peptides as a preliminary measure of their potential in vivo applicability.

The acute in vivo toxicity testing was performed via intravenous tail vein injection of solutions containing representative peptides of n = 2 [$(IRIK)_2$-NH_2] and n = 3 [$(IRVK)_3$-NH_2] repeat units in mice. The former was selected due to its superior SI among peptides with n = 2 repeat units, while the latter was chosen due to its better antimicrobial activities, selectivities and endotoxin neutralization properties (to be discussed later) among peptides with n = 3 repeat units. $(IRIK)_2$-NH_2 and $(IRVK)_3$-NH_2 were respectively found to have lethal dose, 50% (LD50; dose required to kill 50% of mice after a specific test period) values of 35.2 mg/kg. The LD50 values of the designed peptides contrast favorably with that of polymyxin B (5.4 mg/kg) and gramicidin (1.5 mg/kg).[30]

2.3. Antimicrobial Mechanisms

To elucidate the antimicrobial mechanism, colony counting experiments were performed after treating the panel of 5 microorganisms with different concentrations of $(IRIK)_2$-NH_2. For each of the microorganisms tested, the peptide achieved killing efficiencies of more than 99.9% (>3 log reductions in colony counts) at the respective MIC values, hence supporting a bactericidal mechanism (Supporting Information Figure S2). The surface morphologies of *E. coli* and *S. aureus* after treatment with $(IRIK)_2$-NH_2 and $(IRVK)_3$-NH_2 were investigated under field-emission scanning electron microscopy (FE-SEM). As shown in **Figure 3**, significant membrane corrugation and damage was observed in *E. coli* and *S. aureus* treated for 2 h with an above MIC concentration (125 mg L^{-1}) of the peptides as opposed to the relatively smooth and intact surfaces of the respective control samples treated with broth containing 10% (by volume) of water. This observation is consistent with the membrane lytic mechanism of the various naturally occurring and synthetic AMPs reported in the literature. Compared to conventional antibiotics that inhibit various targets within the biosynthetic pathways of microorganisms, the rapid physical disruption of microbial cell membranes by the peptides is expected to provide an inherent advantage in the clinical setting due to the reduced likelihood for the development of mutations that confer multidrug resistance.

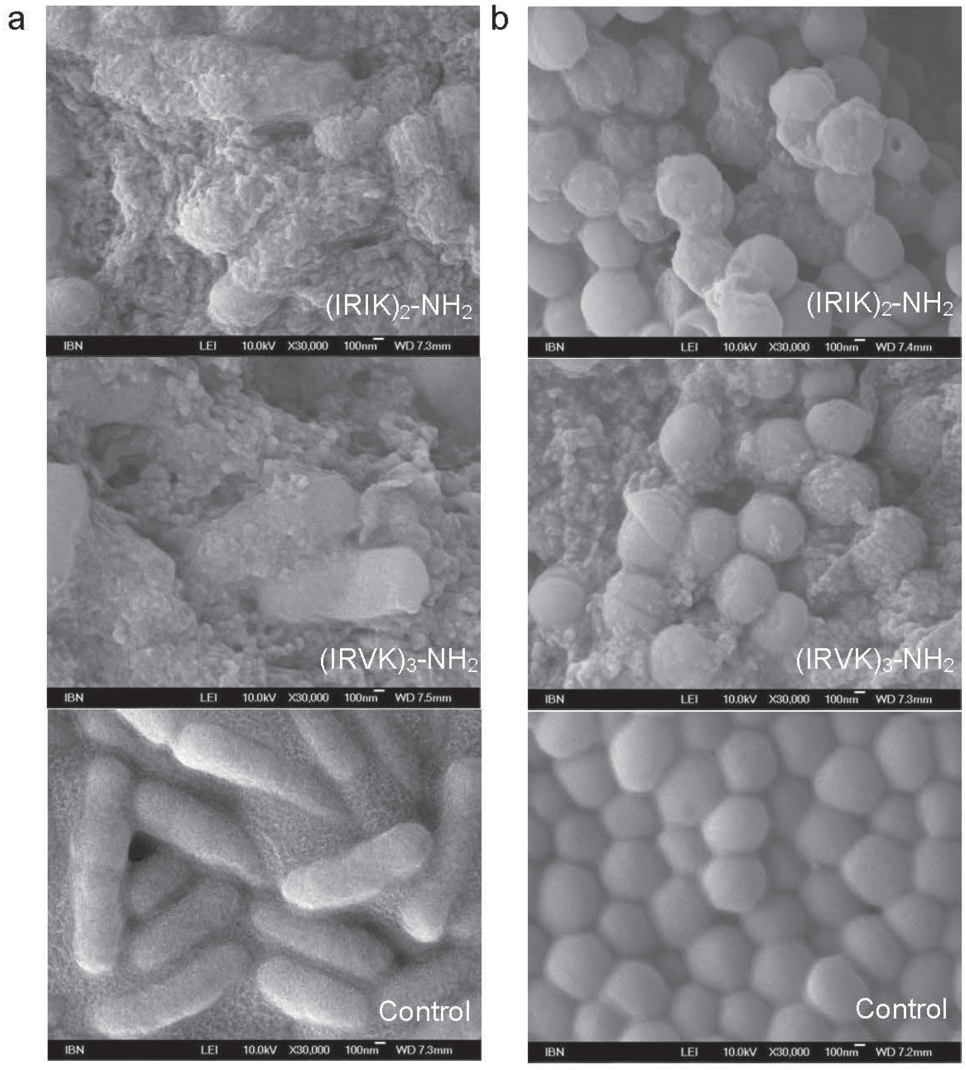

Figure 3. FE-SEM images showing extensive damage to a) *E. coli* and b) *S. aureus* membranes after 2 h treatment with $(IRIK)_2$-NH_2 and $(IRVK)_3$-NH_2 (125 mg L^{-1}) in contrast to the intact surfaces of respective controls incubated with broth containing 10% (by volume) of water.

2.4. Antibiofilm Activities

We next investigated the anti-biofilm ability of the synthetic antimicrobial peptides on pre-formed biofilms, which are intrinsically more challenging than the prevention of biofilm formation. As shown in **Figure 4**a, $(IRIK)_2$-NH_2 and $(IRVK)_3$-NH_2 demonstrated a dose-dependent inhibition of *S. aureus* growth in biofilms. $(IRIK)_2$-NH_2 was found to induce significantly higher reduction in cell viabilities across the three concentrations tested ($P < 0.01$), with cell viability drastically reduced to less than 10% at 4 × MIC level within 24 h. To determine the relative amounts of biomass remaining after treatment with the peptides, crystal violet staining and solubilization of the biofilms were performed. Similar to the decrease in *S. aureus* cell viability, the amount of biomass in the treated biofilms was also observed to be reduced in a dose-dependent manner (Figure 4b). The changes in the amount of biomass after treatment with $(IRIK)_2$-NH_2 were further investigated under FE-SEM. As seen in Figure 4c, the microbial cell densities in the biofilms decreased with increasing peptide concentrations, with a greater degree of membrane disruption observed at 4 × MIC and 8 × MIC concentrations. This observation is consistent with both the reduction in cell viabilities and biomass observed earlier. These results, taken together, thus provide direct evidence that the 8 and 12 amino acids long peptides are able to kill microbes embedded within biofilms and efficiently mediate the dispersion of biofilm matrices.

2.5. Endotoxin Neutralization Activities

The lipopolysaccharide (LPS) endotoxin, which has potent immunostimulating properties is an integral structural component in the outer membrane leaflet of Gram-negative bacteria.

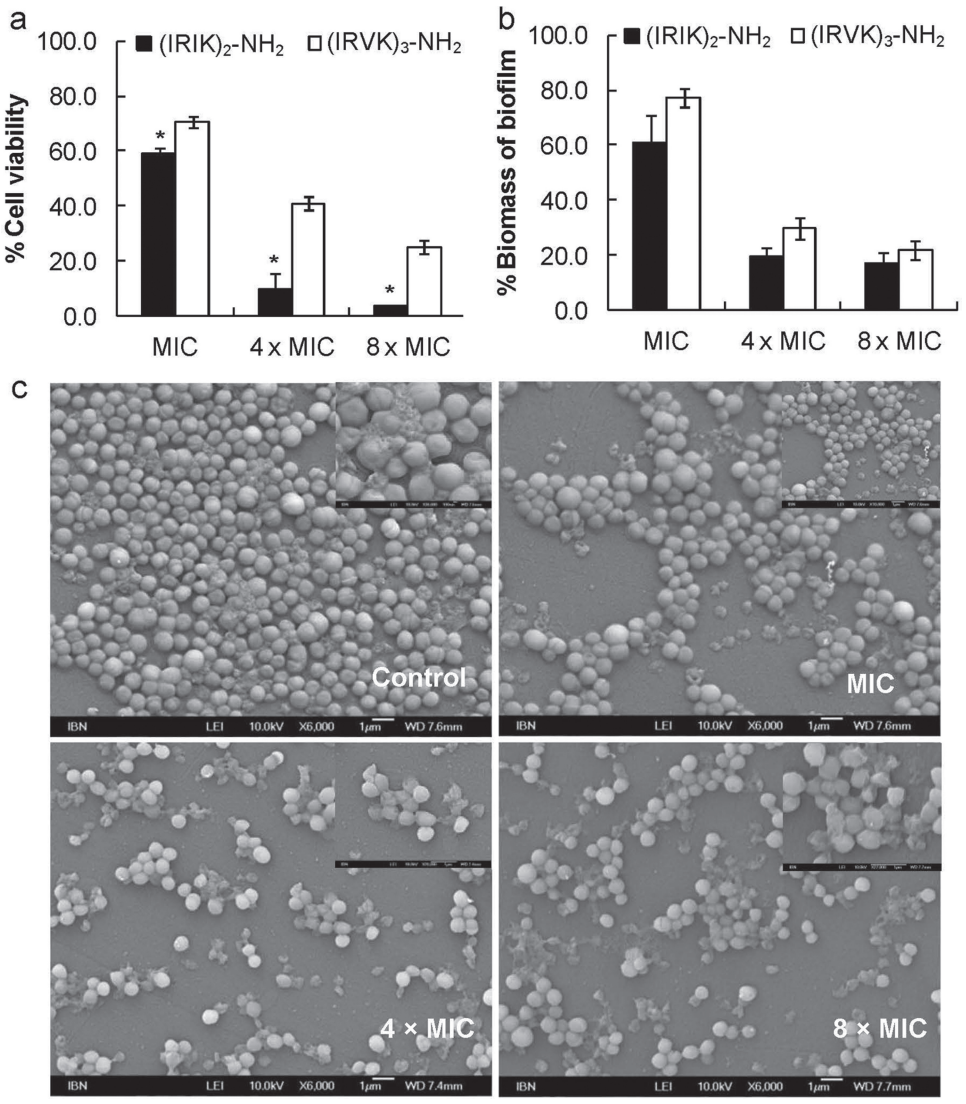

Figure 4. Antibiofilm activities of β-sheet forming peptides. a) Cell viability and b) biomass of *S. aureus* biofilms were reduced after 24 h treatment with various concentrations of $(IRIK)_2$-NH_2 and $(IRVK)_3$-NH_2 relative to the untreated control. c) FE-SEM images of *S. aureus* biofilms treated with the indicated concentrations of $(IRIK)_2$-NH_2. A greater reduction in bacteria cell density and increased membrane damage were observed at 4 × and 8 × MIC values. Size of scale bars: 1 μm. $* P < 0.01$ relative to $(IRVK)_3$-NH_2 at the indicated concentration.

As the anionic amphiphilic lipid A domain is well-regarded as the active moiety of LPS, cationic antimicrobial peptide amphiphiles present as particularly useful candidates for binding and neutralizing of LPS via electrostatic interactions with the anionic head group by cationic lysine or arginine residues, and dissociation of LPS aggregates via hydrophobic interactions between the alkyl chains of LPS and non-polar amino acid side chains. In order to evaluate the ability of the designed synthetic peptides to bind and dissociate LPS aggregates, we incubated FITC-conjugated LPS with the various peptides and monitored the changes in fluorescent intensities over 2 h. In aqueous solutions, FITC sequestered within LPS aggregates exhibit self-quenching, resulting in low fluorescent intensities.[31] Conversely, when FITC-LPS aggregates dissociate, the fluorescence increases due to a dequenching effect. As seen in **Figure 5**a, β-sheet forming peptides with n = 2 did not seem to induce discernible disruption of FITC-LPS aggregates as evident from the lack of changes in fluorescent intensity up to peptide concentrations of 500 mg L^{-1}. The corresponding peptides with 3 repeat units, however, produced a strong dose-dependent enhancement in the fluorescent intensities of FITC-LPS (Figure 5b), clearly demonstrating the requirement for a minimum peptide length for the disruption of FTIC-LPS aggregates. Among the three β-sheet forming peptides with n = 3, the peptides that induced a greater percentage change in fluorescent intensities at lower concentrations followed the order: $(IRIK)_3$-NH_2 > $(IRVK)_3$-NH_2 > $(VRVK)_3$-NH_2. This result suggests that the overall hydrophobicity of the peptides influence the destabilization of the FTIC-LPS aggregates, with the peptide containing a greater amount of the slightly more hydrophobic

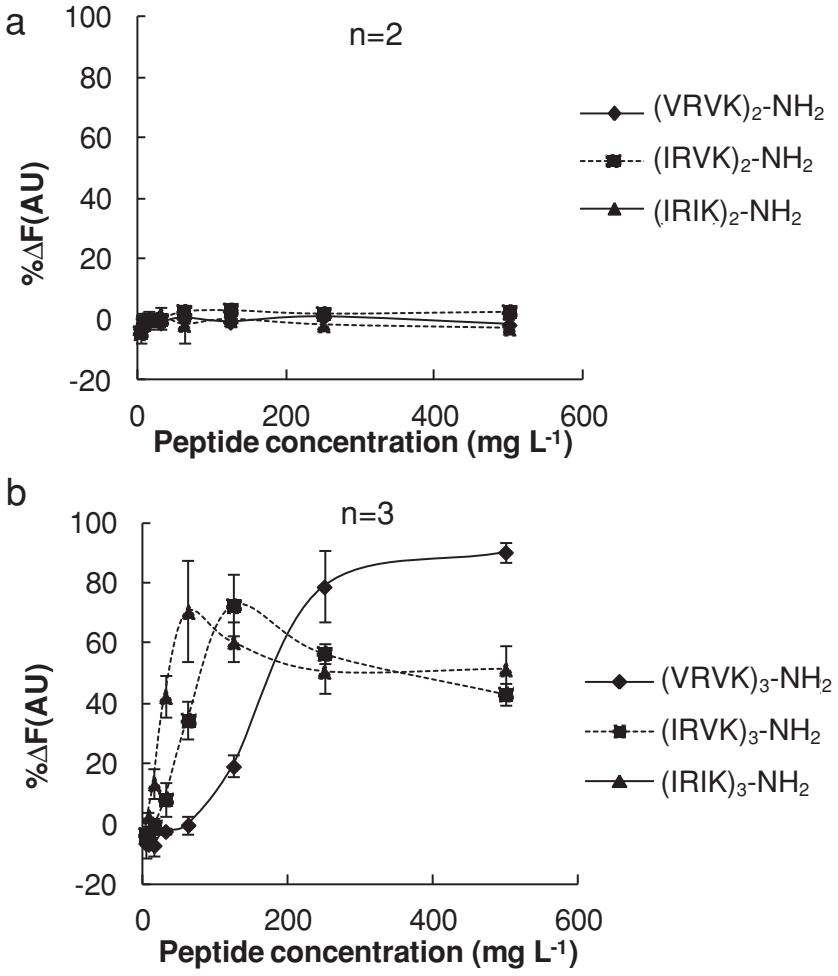

Figure 5. Effects of β-sheet forming antimicrobial peptides with a) two repeat units (n = 2) and b) three repeat units (n = 3) on the stability of FITC-labeled LPS aggregates. The designed antimicrobial peptides with n = 3 repeat units effectively mediated disruption of FITC-LPS aggregates.

Ile residues being more effective at disrupting FITC-LPS aggregates.

The endotoxin neutralizing capabilities of the synthetic peptides were established by stimulating the rat macrophage cell line NR8383 with 100 ng mL^{-1} LPS in the presence of various peptides. Nitric oxide is a pro-inflammatory mediator that is secreted by activated mononuclear phagocytes, including monocytes and macrophages in the presence of LPS. Due to the short half-life of nitric oxide in oxygen-containing aqueous medium, the amount released by the activated macrophages was estimated via quantification of the more stable NO metabolite, nitrite[32] in the cell culture media. A reduction in nitrite levels secreted by LPS-stimulated macrophages in the presence of the β-sheet forming peptides when compared to the non-treated control thus indicates LPS neutralization. As seen from **Figure 6**a, the peptides were found to effectively inhibit LPS-stimulated NO production, with significantly decreased nitrite concentrations compared to the non-peptide treated control even at a low peptide concentration of 15.6 mg L^{-1}. The degree of LPS neutralization mediated by the various peptides was in the order of $(IRIK)_3$-NH_2 > $(IRVK)_3$-NH_2 > $(VRVK)_3$-NH_2, which was in close agreement with the trend observed earlier in the FITC-LPS interaction assay. Importantly, at 125 mg L^{-1} of $(IRIK)_3$-NH_2 and $(IRVK)_3$-NH_2, the nitrite concentration was reduced to the control level. We further evaluated the cytotoxicities of the peptides against the NR8383 cell line and found that the cell viabilities was in excess of 80% up to concentrations of 62.5, 125, and 125 mg L^{-1} for $(VRVK)_3$-NH_2, $(IRVK)_3$-NH_2 and $(IRIK)_3$-NH_2, respectively (Figure 6b). These results confirmed that the good anti-inflammatory properties of the synthetic peptides were independent of their effects on cell viability and that the peptides were not cytotoxic, indicating their suitability for systemic administration. Although $(IRIK)_3$-NH_2 possessed the most potent anti-inflammatory activity among the three peptides, its relatively weak antimicrobial activities (GM MIC value = 162.7 mg L^{-1}) and lower selectivity index (SI = 3.1) suggests that the second best anti-inflammatory peptide $(IRVK)_3$-NH_2, which has a much lower geometric mean MIC value of 47.3 and higher selectivity index of 26.4 (Table 2), is a more suitable candidate for the safe and efficacious treatment of bloodstream infections.

3. Conclusions

In this study, a series of short synthetic β-sheet folding antimicrobial peptides was designed based upon a basic principle of having amphiphatic dyad repeats of cationic and hydrophobic amino acid residues with high β-sheet folding propensities. The designed β-sheet folding peptides demonstrated broad spectrum antimicrobial activities against Gram-positive *S. epidermidis* and *S. aureus*, Gram-negative *E. coli* and *P. aeruginosa* as well as yeast *C. albicans*. Optimal peptide sequences of n = 2 and n = 3 repeat units, namely $(IRIK)_2$-NH_2 and $(IRVK)_3$-NH_2, were found to possess high selectivity indices of 44.8 and 26.4, respectively. Acute in vivo toxicity testing in mice revealed higher intravenous LD50 values for the optimal synthetic peptides as compared to the clinically used polymyxin B and gramicidin. The optimal peptides sequences also demonstrated efficient inhibition of sessile biofilm bacterial growth and biomass dispersal. Additionally, synthetic peptides with 3 repeat units, including $(VRVK)_3$-NH_2, $(IRVK)_3$-NH_2 and $(IRIK)_3$-NH_2, demonstrated endotoxin binding and neutralizing capabilities with minimal or no cytotoxicities induced at the concentrations required for functional effects. Taken together, our findings clearly demonstrated that the rationally designed synthetic β-sheet folding peptides are highly selective and have potential for use as broad spectrum antimicrobial agents to overcome the prevalent problem of multidrug resistance in a wide range of

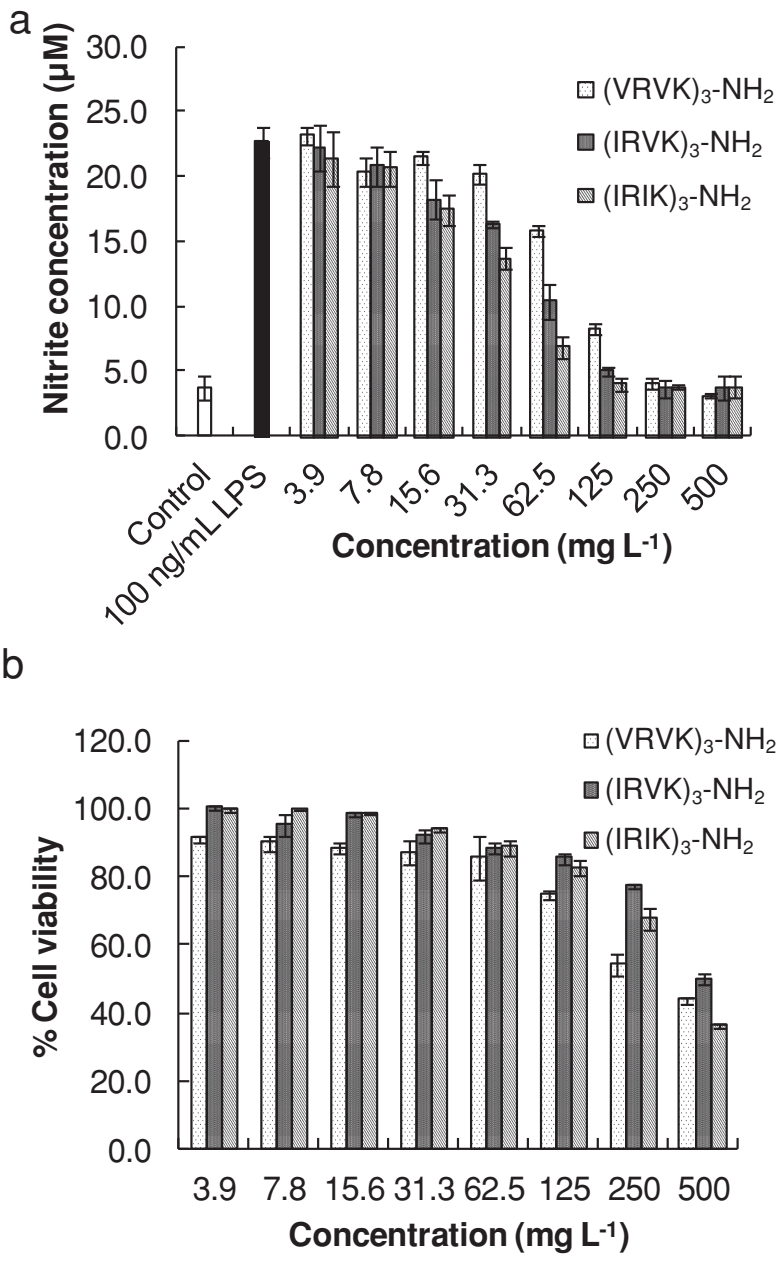

Figure 6. Effect of synthetic β-sheet forming antimicrobial peptides on a) LPS-stimulated NO production and b) viability of NR8383 rat macrophage cells after 18 h incubation with various concentrations of the designed antimicrobial peptides.

bacterial- or fungal-associated infectious disease applications including, but not limited to, the prevention and eradication of therapeutically challenging biofilms on open wounds, catheters or implants and the neutralization of microbial endotoxins for improved treatment of bloodstream infections.

4. Experimental Section

Materials: Peptides used in this study were synthesized by GL Biochem (Shanghai, China) and purified to more than 95% using reverse phase (RP)-HPLC. The molecular weights of the peptides were further confirmed using matrix-assisted laser desorption/ionization time-of-flight mass spectroscopy (MALDI-TOF MS, Model Autoflex II, Bruker Daltonics Inc., U.S.A.) using α-cyano-4-hydroxycinnamic acid (4-HCCA) as matrix. 4-HCCA was purchased from Sigma-Aldrich (Singapore) and used in saturated acetonitrile/water (1:1 volume ratio) after re-crystallization. Phosphate-buffered saline (10 × PBS) was purchased from 1st Base (Singapore) and diluted to the intended concentration before use. Mueller-Hinton Broth II (cation-adjusted; MHB II) and yeast mould broth (YMB) powders were purchased from BD Diagnostics (Singapore) and re-constituted according to the manufacturer's instructions. *Staphylococcus epidermidis* (ATCC No. 12228), *Staphylococcus aureus* (ATCC No. 29737), *Escherichia coli* (ATCC No. 25922), *Pseudomonas aeruginosa* (ATCC No. 9027) and yeast *Candida albicans* (ATCC No. 10231) were obtained from ATCC (U.S.A) and cultivated according to the recommended protocols. Polymyxin B sulfate (meets USP testing specifications), lipopolysaccharide (LPS) and FITC-conjugated LPS from *E. coli* 0111:B4 were purchased from Sigma-Aldrich. Griess reagent system was obtained from Promega (USA) and used according to the manufacturer's protocol.

Circular Dichroism (CD) Spectroscopy: Each peptide was first dissolved at 0.5 mg mL^{-1} in deionized (DI) water alone or DI water containing 25 mM of SDS surfactant. The CD spectra were recorded at room temperature with a CD spectropolarimeter (JASCO Corp. J-810), using a quartz cell with 1.0 mm path length. CD spectra were acquired with solvent subtraction from 190 to 240 nm at 10 nm min^{-1} scanning speed and were averaged from 5 runs per peptide sample. The acquired CD spectra were converted to mean residue ellipticity using the following equation:

$$\theta M = \frac{\theta obs}{10} \cdot \frac{MRW}{c \cdot l}$$

where θ_M refers to the mean residue ellipticity (deg cm^2 dmol^{-1}), θ_{obs} is the observed ellipticity corrected for DI water at a given wavelength (mdeg), MRW is the residue molecular weight (M_w · number of amino acid residues^{-1}), c is the peptide concentration (mg mL^{-1}), and l is the path length (cm).

Minimal Inhibitory Concentration (MIC) Measurements: The antimicrobial activities of the peptides and polymyxin B sulfate were investigated against Gram-positive *S. epidermidis* and *S. aureus*, Gram-negative *E. coli* and *P. aeruginosa*, and yeast *C. albicans* using the broth microdilution method. Bacterial cells were cultivated in MHBII at 37 °C and yeast cells were grown in YMB at room temperature under constant shaking at 300 rpm to reach mid-logarithmic growth phase. The microbial suspensions were diluted with the appropriate broths and adjusted to give an initial optical density (O.D.) reading of approximately 0.07 at a wavelength of 600 nm on a microplate reader (TECAN, Switzerland), which corresponds to McFarland Standard No. 1 (approximately 3 × 10^8 CFU mL^{-1}). Peptides and polymyxin B sulfate were dissolved in 0.2 μm filtered HPLC grade water and subjected to a series of two-fold dilutions using the appropriate broths. 100 μL of microorganism suspension with an initial loading level of 3 × 10^5 CFU mL^{-1} was added to an equal volume (100 μL) of peptide solution to achieve final concentrations ranging from 3.9 to 500 mg L^{-1} and with water concentration fixed at 10% (by volume) in each well of a 96-well plate.

After 18 or 42 h incubation with shaking at 37 °C or room temperature for bacteria and yeast, respectively, the MIC was taken as the lowest polymer concentration at which no microbial growth was observed visually and with no change in O.D. reading from 0 h. Microbial cells in broth containing 10% (by volume) of HPLC grade water as well as pure broth alone were used as the negative controls. To ascertain aseptic handling, wells containing pure broth without microbes were included in each experiment. Each test was performed in 6 replicates on at least 2 independent occasions.

Hemolysis Testing: Fresh rat red blood cells were subjected to 25 × dilution with PBS to obtain an approximate 4% (by volume) suspension for use in this experiment. 300 μL of red blood cell suspension was added to each tube containing equal volume (300 μL) of peptide and polymyxin B sulfate solutions in PBS. The tubes were incubated at 37 °C for 1 h before subjected to centrifugation at 1000 × g for 5 min. Aliquots (100 μL) of supernatant were transferred to each well of a 96-well plate and analyzed for hemoglobin release at 576 nm using a microplate reader (TECAN, Switzerland). Red blood cells suspension incubated with PBS was used as negative control. Absorbance of red blood cells lyzed with 0.1% v/v Triton X-100 was used as the positive control and taken to be 100% hemolytic. Percentage of hemolysis was calculated using the following formula: Hemolysis (%) = [(O.D.576 nm of treated sample − O.D.576 nm of negative control)/(O.D.576 nm of positive control − O.D.576 nm of negative control)] × 100. Data are expressed as mean ± standard deviations of 4 replicates.

Acute In Vivo Toxicity Testing: Animal studies were performed according to protocols approved by the Singapore Biological Research Center (BRC)'s Institutional Animal Care and Use Committee. The LD50 values were determined using female Balb/c mice (6–7 weeks old, 18–22 g) according to the Up-and-Down-Procedure described in the Organisation for Economic Cooperation and Development Guideline for the Testing of Chemicals (OECD 425). The animals were allowed to acclimatize for 5 days and then randomly distributed into groups. $(IRIK)_2$-NH_2 and $(IRVK)_3$-NH_2 were dissolved in 0.2 μm filtered HPLC grade water, diluted using sterile PBS (pH 7.4) and administered via tail vein injection at specific doses (i.e., 17.6 and 56 mg/kg, 0.1 mL). Mortality was monitored for 14 days post-injection and LD50 was determined using the maximum likelihood method.

Field Emission-Scanning Electron Microscopy (FE-SEM) Imaging: *E. coli* and *S. aureus* suspensions at ≈3×10^8 CFU ml^{-1} (100 μL) were incubated with an equal volume of broth containing 20% (by volume) of water and a lethal dose (125 mg L^{-1}) of a representative peptide in a 96 well-plate for 2 h. Eight replicates of each condition was pooled into a microfuge tube, pelleted down at 4000 rpm for 5 min, and rinsed twice with PBS. The samples were then fixed with 4% formaldehyde at room temperature for 15 min, followed by rinsing with DI water. Dehydration of the cells was performed using a series of graded ethanol solutions (35, 50, 75, 90, 95, and 100%). The samples were mounted on carbon tape, allowed to air-dry and sputter coated with platinum before imaging using a FE-SEM setup (JEOL JSM-7400F, Japan).

Biofilm Growth Inhibition, Biomass Assay and Biofilm Imaging: Overnight cultures of *S. aureus* diluted to 3×10^6 CFU ml^{-1} were added into each well of a 96-well plate at a volume of 100 μL per well and allowed to adhere overnight at 37 °C with gentle shaking at 100 rpm. The wells were then rinsed once with 100 μL of PBS to remove planktonic cells and loosely attached cells, and replenished with 100 μL of fresh broth. Biofilm formation was allowed to proceed up to 6–8 days with daily rinsing and media changes before use in experiments. To determine the effects of peptide treatment on viability of *S. aureus* in biofilms, 100 μL of $(IRIK)_2$-NH_2 and $(IRVK)_3$-NH_2 solutions at MIC, 4 × MIC and 8 × MIC levels were added into each well and allowed to incubate for 24 h. Subsequently, the solutions were removed, rinsed once with 100 μL of PBS before 120 μL of activated XTT solution was added into each well. After 4 h incubation, 90 μL aliquots from each well was transferred to a new 96-well plate for the determination of absorbance using a microplate reader (TECAN, Switzerland) at measurement and reference wavelengths of 490 nm and 660 nm, respectively. Relative cell viability was expressed as $[(A_{490\ nm}\text{-}A_{660\ nm})\text{sample}/(A_{490\ nm}\text{-}A_{660\ nm})\text{control}] \times 100\%$. Data are expressed as mean ± standard deviations of four replicates per concentration.

The biomass of the biofilms was estimated by a crystal violet staining assay. Briefly, the formed biofilms were first treated with the peptides for 24 h as described above. After aspirating the culture medium, the biofilms were rinsed once with PBS, fixed with methanol for 15 min at room temperature and stained with 100 μL of 0.1% (weight by volume) crystal violet for 10 min. The excess crystal violet dye was removed by rinsing the wells with DI water for five times. The dye that is associated with the biofilm was extracted using 100 μL of 33% glacial acetic acid per well and 60 μL aliquot from each well was transferred to a new 96-well plate for quantification of absorbance at a wavelength of 570 nm using a microplate reader (TECAN, Switzerland). The relative amount of biomass remaining after peptide treatment was expressed as a percentage of the control treated with broth containing 10% (by volume) of water. Data represent mean ± standard deviations of four replicates per concentration.

After 24 h treatment with $(IRIK)_2$-NH_2 at MIC, 4 × MIC and 8 × MIC concentrations, residual biofilms were rinsed with PBS, fixed with 4% formaldehyde and then subjected to dehydration using a series of graded ethanol solutions as described above. The bottom of the 96-well plate was removed, mounted on carbon tape and sputter coated with platinum before imaging using a FE-SEM setup (JEOL JSM-7400F, Japan).

FITC-LPS Binding Assay: 50 μL of 1 μg mL^{-1} FITC-LPS in PBS was treated with an equal volume of peptide solution (50 μL) in each well of a black 96-well plate with clear bottom. The interactions of the peptides with the FITC-conjugated LPS were studied by exciting the FITC-LPS at 480 nm and monitoring the emission of FITC at 516 nm in the presence of increasing concentrations of peptides (3.9, 7.8, 15.6, 31.3, 62.5, 125, 250, 500 mg L^{-1}) using a fluorescence microplate reader (TECAN, Switzerland) at 0 h and 2 h. 100 μL of PBS containing 10% by volume of water was included as a blank. Fluorescence intensity of 100 μL FITC-LPS (0.5 μg mL^{-1}) in PBS was used a negative control. The percentage change in fluorescence intensity was calculated as follows: $\%\Delta F(AU) = [((F_{Sample}\text{-}F_{Blank})/(F_{Control}\text{-}F_{Blank})) \times 100]\text{–}100$. Results are expressed as mean ± standard deviations of 4 replicates.

Cell Culture: The rat macrophage cell line NR8383 was maintained in F12 growth medium supplemented with 2 mM L-glutamine, 1.5 g L^{-1} sodium bicarbonate and 15% FBS and cultured at 37 °C under an atmosphere of 5% CO_2 and 95% humidified air.

Endotoxin Neutralization Assay: NR8383 cells were plated at a density of 4×10^4 and stimulated with LPS (100 ng mL^{-1}) from *E. coli* 0111:B4 in the presence (3.9, 7.8, 15.6, 31.3, 62.5, 125, 250, 500 mg L^{-1}) or absence of peptides in each well of a 96-well plate for 18 h at 37°C. Untreated cells and cells that were stimulated with LPS alone served as the positive and negative controls, respectively. The amount of NO produced was estimated by quantifying the concentration of the stable NO metabolite nitrite in the isolated supernatant fractions using the Griess reagent (1% sulfanilamide, 0.1% N-1-napthylethylenediamine dihydrochloride, 5% phosphoric acid) according to the manufacturer's protocol. The absorbance was measured at 540 nm and nitrite concentrations were determined using a standard reference curve prepared from known concentrations of $NaNO_2$ solutions.

Cytotoxicity Testing: The rat macrophage cell line NR8383 was seeded at a density of 4×10^4 cells per well of a 96-well plate and treated with increasing concentrations of peptides (3.9, 7.8, 15.6, 31.3, 62.5, 125, 250, 500 mg L^{-1}) for 18 h at 37 °C. Subsequently, 20 μL of CellTitre-Blue reagent was added into each well and the plate was incubated for a further 4 h. The fluorescence intensity readings of the wells were determined at excitation wavelength of 560 nm and emission wavelength of 590 nm using a microplate reader. Control wells containing peptide solutions at the respective concentrations in the absence of cells were included to determine background fluorescence.% Cell viability = $[(F_{treated\ sample} - F_{corresponding\ background})/(F_{10\%\ water\ control} - F_{10\%\ water\ control\ background})] \times 100$. Data are expressed as mean ± standard deviations of 4 replicates.

Supporting Information

Supporting Information is available from the Wiley Online Library or from the author.

Acknowledgements

This work was funded by the Institute of Bioengineering and Nanotechnology, Biomedical Research Council, Agency for Science, Technology and Research, Singapore.

Received: September 30, 2012
Revised: December 17, 2012
Published online: February 26, 2013

[1] C. Mathers, D. M. Fat, J. Boerma, *The global burden of disease: 2004 update*, World Health Organization, 2008.
[2] S. C. Park, Y. Park, K. S. Hahm, *Int. J. Mol. Sci.* **2011**, *12*, 5971.
[3] S. L. Percival, C. Emanuel, K. F. Cutting, D. W. Williams, *Int. Wound J.* **2012**, *9*, 14.
[4] C. I. Kang, S. H. Kim, W. B. Park, K. D. Lee, H. B. Kim, E. C. Kim, M. Oh, K. W. Choe, *Antimicrob. Agents Chemother.* **2005**, *49*, 760.
[5] S. A. David, *J. Mol. Recognit.* **2001**, *14*, 370.
[6] B. Spellberg, R. Guidos, D. Gilbert, J. Bradley, H. W. Boucher, W. M. Scheld, J. G. Bartlett, J. Edwards, *Clin. Infect. Dis.* **2008**, *46*, 155.
[7] M. N. Melo, R. Ferre, M. A. R. B. Castanho, *Nat. Rev. Microbiol.* **2009**, *7*, 245.
[8] G. Wang, X. Li, Z. Wang, *Nucleic Acids Res.* **2009**, *37*, D933.
[9] R. E. W. Hancock, H. G. Sahl, *Nat. Biotechnol.* **2006**, *24*, 1551.
[10] L. T. Nguyen, J. K. Chau, N. A. Perry, L. de Boer, S. A. J. Zaat, H. J. Vogel, *PLoS One* **2010**, *5*, e12684.
[11] A. Pellegrini, R. von Fellenberg, *Biochim. Biophys. Acta Protein Struct. Mol. Enzymol.* **1999**, *1433*, 122.
[12] D. Lee, J. Powers, K. Pflegerl, M. Vasil, R. Hancock, R. Hodges, *J. Pept. Res.* **2004**, *63*, 69.
[13] T. Godballe, L. L. Nilsson, P. D. Petersen, H. Jenssen, *Chem. Biol. Drug Des.* **2011**, *77*, 107.
[14] H. Meng, K. Kumar, *J. Am. Chem. Soc.* **2007**, *129*, 15615.
[15] G. Bell, P. H. Gouyon, *Microbiology* **2003**, *149*, 1367.
[16] N. Wiradharma, U. Khoe, C. A. E. Hauser, S. V. Seow, S. Zhang, Y. Y. Yang, *Biomaterials* **2011**, *32*, 2204.
[17] Z. Jiang, A. I. Vasil, J. D. Hale, R. E. W. Hancock, M. L. Vasil, R. S. Hodges, *Pept. Sci.* **2008**, *90*, 369.
[18] Z. Jiang, A. I. Vasil, L. Gera, M. L. Vasil, R. S. Hodges, *Chem. Biol. Drug Des.* **2011**, *77*, 225.
[19] Y. Jin, J. Hammer, M. Pate, Y. Zhang, F. Zhu, E. Zmuda, J. Blazyk, *Antimicrob. Agents Chemother.* **2005**, *49*, 4957.
[20] W. C. Wimley, *Protein Sci.* **2002**, *11*, 301.
[21] D. L. Minor Jr., P. S. Kim, *Nature* **1994**, *367*, 660.
[22] C. K. Smith, J. M. Withka, L. Regan, *Biochemistry (Moscow)* **1994**, *33*, 5510.
[23] K. H. Mayo, E. Ilyina, H. Park, *Protein Sci.* **1996**, *5*, 1301.
[24] P. Bulet, R. Stöcklin, L. Menin, *Immunol. Rev.* **2004**, *198*, 169.
[25] M. Pasupuleti, A. Schmidtchen, M. Malmsten, *Crit. Rev. Biotechnol.* **2012**, 32, 143.
[26] Y. H. Nan, S. H. Lee, H. J. Kim, S. Y. Shin, *Peptides* **2010**, *31*, 1826.
[27] A. A. Langham, H. Khandelia, Y. N. Kaznessis, *Pept. Sci.* **2006**, *84*, 219.
[28] C. Ried, C. Wahl, T. Miethke, G. Wellnhofer, C. Landgraf, J. Schneider-Mergener, A. Hoess, *J. Biol. Chem.* **1996**, *271*, 28120.
[29] A. P. Zavascki, L. Z. Goldani, J. Li, R. L. Nation, *J. Antimicrob. Chemother.* **2007**, *60*, 1206.
[30] Neomycin and Polymyxin B Sulfates and Gramicidin Ophthalmic Solution USP; MSDS No. 034; Gary Wong: Tampa, FL, May 13, 2004.
[31] Y. Rosenfeld, N. Papo, Y. Shai, *J. Biol. Chem.* **2006**, *281*, 1636.
[32] L. J. Ignarro, J. M. Fukuto, J. M. Griscavage, N. E. Rogers, R. E. Byrns, *Proc. Natl. Acad. Sci. USA* **1993**, *90*, 8103.